Y-chromosome variation and Irish origins

A pre-neolithic gene gradation starts in the near East and culminates in western Ireland.

Ireland's position on the western edge of Europe suggests that the genetics of its population should have been relatively undisturbed by the demographic movements that have shaped variation on the mainland. We have typed 221 Y chromosomes from Irish males for seven (slowly evolving) biallelic and six (quickly evolving) simple tandem-repeat markers. When these samples are partitioned by surname, we find significant differences in genetic frequency between those of Irish Gaelic and of foreign origin, and also between those of eastern and western Irish origin. Connaught, the westernmost Irish province, lies at the geographical and genetic extreme of a Europe-wide cline.

Surnames have been used in Ireland from about AD 950 as markers of complex local kinship systems. As both surnames and Y chromosomes are paternally inherited, we divided our Irish sample into seven surname cohorts for which ancient geographical information is known, with some error. Four are of prehistoric, Gaelic origin (Ulster, Munster, Leinster and Connaught) and three are diagnostic of historical influx (Scottish, Norman/Norse and English)[1].

The biallelic markers (*SRY-1532*, *M9*, *YAP*, *SRY-2627* (ref. 2); *SRY-8299* (ref. 3); *sY81* (ref. 4); and *92R7* (ref. 5)) define nine haplogroups (clusters of genetic variants) which are highly non-randomly distributed among human populations[6], including our samples. In particular, haplogroup 1 (hg 1) has a very high frequency in Ireland (78.1% in the island as a whole).

Surname subdivision reveals a cline in Irish samples, with exogenous samples clearly showing lower frequencies (English, 62.5%; Scottish, 52.9%; Norman/Norse, 83.0%) than Gaelic Irish samples (Leinster, 73.3%; Ulster, 81.1%; Munster, 94.6%),
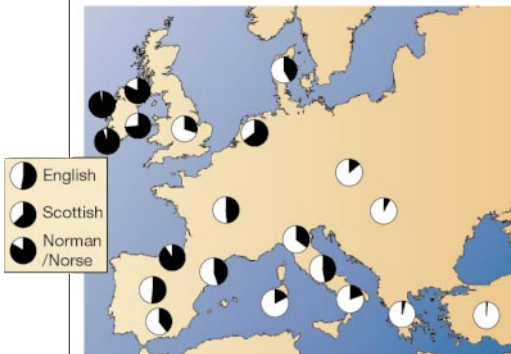

Figure 1 Distribution of observed and estimated haplogroup 1 Y-chromosome haplotypes in Europe. A cline stretches from a frequency of 1.8% in Turkey to peaks in the Basque country (89%) and the west of Ireland (98% in Connaught, the westernmost marker).
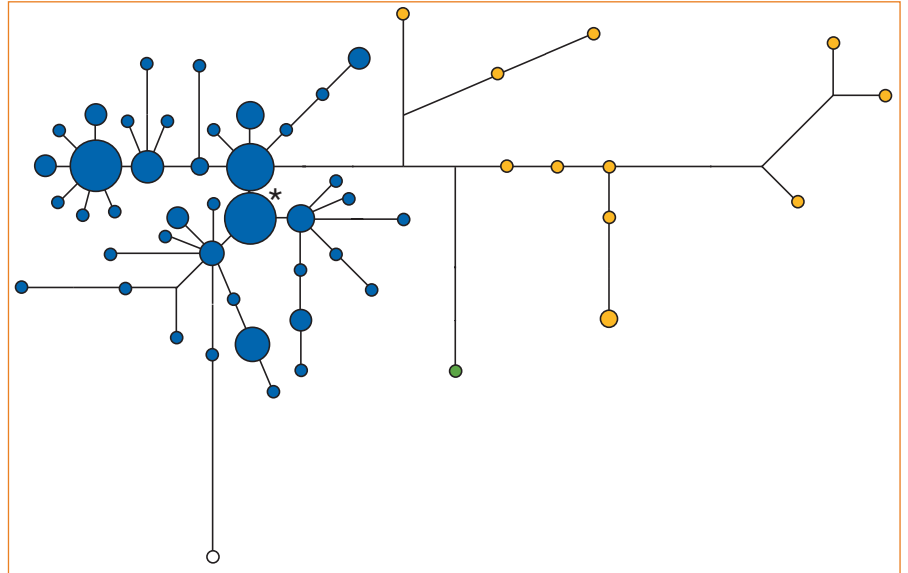

Figure 2 Consensus maximum parsimony networks of Irish Gaelic haplotypes summarizing both single tandem-repeat (*DYS19, DYS3891, DYS390, DYS391, DYS392 and DYS393*; ref. 14) and biallelic variation. Branch lengths are proportional to the number of mutational steps and node areas are proportional to haplotype frequencies. Haplogroup (hg) 1, blue; hg 2, yellow; hg 21, green; hg 26, white. Asterisk, estimated ancestral haplotype. The separate clustering of haplogroups and the tight clustering of the Irish hg 1 haplotypes around a few numerous, central variants are constant through all most-parsimonious trees and were resistant to repetition of the analysis with randomized inputs.

which almost reach fixation in the westernmost province (Connaught, 98.3%). These highly significant differences in the frequency of hg 1 between Irish Gaelic and non-Gaelic Y chromosomes ($P < 0.001$) and between eastern and western Gaelic Y chromosomes ($P < 0.001$) persist when duplicated surnames are removed.

Eighty per cent ($n = 26$; ref. 7) of European hg 1 Y chromosomes belong to 'haplotype 15', defined by using the complex p49f/*Taq*I polymorphic system[8]. Using this relationship, we estimated that hg 1 frequencies follow a cline within Europe[9], extending from the Near East (1.8% in Turkey) to a peak in the Spanish Basque country (89%; ref. 10) in the west (Fig. 1). This cline mirrors other genetic gradients in Europe and is best explained by the migration of Neolithic farmers from the Near East[9]. When the surname-divided Irish data are appended to this cline, it continues to the western edge of Europe, with hg 1 — the putative pre-Neolithic western European variant — reaching its highest frequency in Connaught (98.3%).

In a maximum-parsimony phylogenetic analysis of both biallellic and simple tandem-repeat (STR) variation between Irish Gaelic haplotypes (Fig. 2), the hg 1 chromosomes cluster together tightly, with the highest-frequency haplotypes occupying central positions, suggesting a coherent common ancestry. The smaller number of non-hg 1 haplotypes shows no such coherence, consistent with their being immigrants. Their concentration in the eastern Gaelic cohorts may be indicative of a prehistoric influx or of later gene flow across the linguistic barrier from historical migrant groups.

These findings suggest that hg 1 is the earlier, indigenous Irish variant. By taking the ancestral haplotype as that with the most common allele for each STR and calculating the average squared distance[11] (assuming a generation time of 27 years and a mutation rate of 0.21%; ref. 12) between it and all variants (Fig. 2), we estimate a date for Irish hg 1 coalescence of 4,200 BP (95% c.i. 1,800–14,800 BP). This relatively recent date (a global estimate of hg 1 coalescence is 30,000 BP; ref. 13) falls well within Ireland's 9,000-year history of human habitation. Although error margins are considerable and include uncertainty related to method, this also provides an upper bound for any agriculturally facilitated population expansion, which, at the fringe of Europe, may have taken place in an insular Mesolithic population of hg 1 genotype.

Emmeline W. Hill*, Mark A. Jobling†, Daniel G. Bradley*

**Department of Genetics, Trinity College, Dublin 2, Ireland*
e-mail: dbradley@mail.tcd.ie
†*Department of Genetics, University of Leicester, University Road, Leicester LE1 7RH, UK*

351

1. MacLysaght, E. *The Surnames of Ireland* (Irish Academic, Dublin, 1997).
2. Hurles, M. E. *et al. Am. J. Hum. Genet.* **63,** 1793–1806 (1998).
3. Whitfield, L. S. *et al. Nature* **378,** 379–380 (1995).
4. Seielstad, M. T. *et al. Hum. Mol. Genet.* **3,** 2159–2161 (1994).
5. Hurles, M. E. *et al. Am. J. Hum. Genet.* **65,** 1437–1448 (1999).
6. Jobling, M. A. & Tyler-Smith, C. *Trends Genet.* **11,** 449–456 (1995).
7. Jobling, M. A. *Hum. Mol. Genet.* **3,** 107–114 (1994).
8. Ngo, K. Y. *et al. Am. J. Hum. Genet.* **38,** 407–418 (1986).
9. Semino, O. *et al. Am. J. Hum. Genet.* **59,** 964–968 (1996).
10. Lucotte, G. & Hazout, S. *J. Mol. Evol.* **42,** 472–475 (1996).
11. Goldstein, D. B. *et al. Proc. Natl Acad. Sci. USA* **92,** 6723–6727 (1995).
12. Heyer, E. *et al. Hum. Mol. Genet.* **6,** 799–803 (1997).
13. Hammer, M. F. *et al. Mol. Biol. Evol.* **15,** 427–441 (1998)
14. Kayser, M. *et al. Int. J. Legal Med.* **110,** 125–133 (1997).

Critical phenomena

Fluctuations caught in the act

When a system approaches a critical point, strong fluctuations develop on every scale, from molecules to the entire system. Here we show that critical fluctuations in the domains in a lipid monolayer can be captured and measured by immobilizing it on a solid support and visualizing the pattern using atomic-force microscopy. Such fluctuations in physical properties may reflect the nanometre-scale domain organization in the lipid-bilayer component of biological membranes.

Large numbers of interacting particles show dramatic phase transitions and critical phenomena. At a critical point, molecular-scale interactions build up to macro-

scopic scales, resulting in universal behaviour[1]. The discovery of critical opalescence at the critical point of carbon dioxide[2], caused by density fluctuations scattering light in the fluid, stimulated attempts to glimpse these fluctuations at all scales.

A monolayer of phospholipids at the interface of air and water can be brought close to a critical point by varying the temperature and surface pressure of the monolayer in a Langmuir trough[3]. We immobilized the monolayer by transferring it, by horizontal dipping, to a solid, hydrophilic substrate of mica using Langmuir–Blodgett techniques[4]. We then imaged critical fluctuations varying in size from nanometres to micrometres using contact-mode atomic-force microscopy.

Figure 1a and b shows two different lipid monolayers — dimyristoyl phosphatidylcholine (DMPC) and dipalmitoyl phosphatidylcholine (DPPC) — close to their critical points. When the monolayer passes through the critical point, the acyl chains of the lipids become disordered and the monolayer becomes thinner. As atomic force microscopy maps the height contours of the monolayer, these images show a monolayer structure with domains of one phase within the other.

The height difference between the two types of domain corresponds to the chain-length difference between an ordered and a disordered lipid acyl chain. Near the critical point, these domains are dynamic and fluctuate strongly when the monolayer is at the air–water interface; we capture them immobilized during the transfer process. The morphology of the domains is very ramified, owing to the vanishing line tension near criticality. Domains of all sizes appear, indicating that there is no characteristic length scale — the hallmark of critical fluctuations.

Figure 1c shows a quantitative analysis of the domain patterns in terms of the structure factor, $S(q)$, where q is the length of a two-dimensional wavevector. The structure-factor data for both DMPC and DPPC scale as a power law, $S(q) \sim q^{-2x}$, with $x \approx 1$. Within the accuracy of the data, this is consistent with the critical-point behaviour associated with the universality class of the two-dimensional Ising model[1].

Lipid domains in monolayers made of phospholipid mixtures can be immobilized

and imaged using similar techniques. Mixtures of phospholipids with acyl chains of different lengths show compositional demixing on the nanometre scale[5].

Monolayers are simple model systems of the lipid bilayer component of cell membranes[6]. Functions supported by lipid bilayers, such as phospholipase activity[7] and protein binding[8], are correlated with lipid-domain formation in the nanometre range that is controlled by the underlying phase transition in the bilayer. Biological membranes contain many different lipid species that are probably organized heterogeneously in the form of domains[9–11] or 'rafts'[12] in the plane of the membrane, though the principles underlying this organization remain largely unknown. Our results suggest that fluctuations in lipid bilayer properties, for example, density or composition, may be responsible for lipid-domain formation in biomembranes.

Lars K. Nielsen*, Thomas Bjørnholm†, Ole G. Mouritsen*
*Department of Chemistry, Technical University of Denmark, DK-2800 Lyngby, Denmark
†CISMI, Laboratory for Materials Science, Department of Chemistry, University of Copenhagen, Fruebjergvej 3, DK-2100 Copenhagen, Denmark
e-mail: ogm@kemi.dtu.dk

1. Stanley, H. E. *Rev. Mod. Phys.* **71,** S358–S366 (1999).
2. Andrews, T. *Phil. Trans. R. Soc. Lond.* **159,** 575–590 (1869).
3. Albrecht, O., Gruler, H. & Sackmann, E. *J. Phys. (Paris)* **39,** 301–313 (1978).
4. Knobler, C. M. & Schwartz, D. K. *Curr. Opin. Colloid Interface Sci.* **4,** 46–51 (1999).
5. Nielsen, L. K., Bjørnholm, T. & Mouritsen, O. G. *J. Phys. Cond. Mat.* **12,** 309–314 (2000).
6. Mouritsen, O. G. & Andersen, O. S. (eds) *Biol. Skr. Kgl. Dan. Vid. Selsk.* **49,** 1–214 (1998).
7. Hønger, T. *et al. Biochemistry* **35,** 9003–9006 (1996).
8. Mustonen, P. *et al. Biochemistry* **26,** 2991–2997 (1987).
9. Mouritsen, O. G. & Jørgensen, K. *Curr. Opin. Struct. Biol.* **7,** 518–527 (1997).
10. Edidin, M. *Curr. Opin. Struct. Biol.* **7,** 528–532 (1997).
11. Korlach, J., Schwille, P., Webb, W. W. & Feigenson, G. W. *Proc. Natl Acad. Sci. USA* **96,** 8461–8466 (1999).
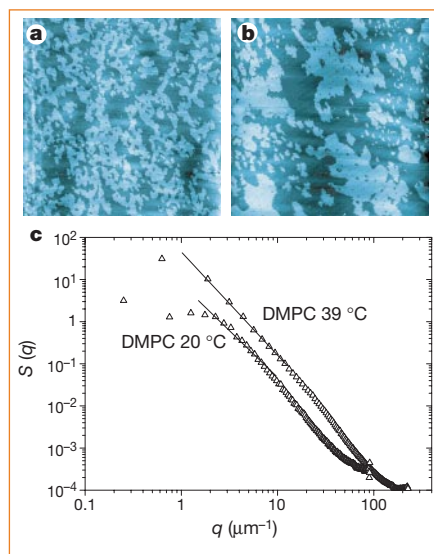12. Simons, K. & Ikonen, E. *Nature* **387,** 569–572 (1997).

Figure 1 Critical fluctuations in phospholipid monolayers imaged by atomic-force microscopy as a height-difference map. **a,b,** Images of dimyristoyl phosphatidylcholine (25×25 μm^2) and dipalmitoyl phosphatidylcholine (20×20 μm^2) monolayers at their respective critical points. The monolayers have been transferred from an air–water interface to solid mica supports. The patterns correspond to lipid domains of one phase immersed into the other. The height difference between the light and dark areas is about 5 Å. **c,** Quantitative analysis of many images like those in **a** and **b** in terms of the structure factor, $S(q)$, in arbitrary units, shown in a double-logaritmic plot as a function of the wavevector, q. The wavevector is related to distance, r, as $q = 2\pi/r$. The data for both phospholipids scale as $S(q) \approx q^{-2x}$, with $x \approx 1$ for $q \lesssim 20$ μm^{-1}. At low q there is a deviation from this power law because of the finite size of the images analysed.

Alzheimer's disease

Apolipoprotein E and cognitive performance

Key proteins implicated in the development of Alzheimer's disease are the β-amyloid precursor protein, which gives rise to the β-amyloid peptides that accumulate in the deteriorating brain[1,2], and the different isoforms of apolipoprotein E (apoE). The apoE4 variant increases the risk of developing the disease compared with apoE3 (ref. 3). We have tested the spatial memory of transgenic mice carrying human forms of these proteins and find that it is impaired in mice with apoE4 but not those with apoE3, even though the levels of β-amyloid in their brains are comparable. The fact that apoE3, but not apoE4,